

Sizing of II-Life Batteries for Grid Support Applications and Economic Evaluations

Giuseppe Graber^a, Vito Calderaro^b, Vincenzo Galdi^c and Antonio Piccolo^d
Department of Industrial Engineering, University of Salerno, Fisciano (SA), Italy

Keywords: Battery Sizing, Economic Assessment, Electric Vehicles, Energy Storage Systems and Second Life.

Abstract: Power systems are facing increasing stress due to modernization changes in both supply, through the growing penetration level of renewable sources, and demand due to the spread diffusion of electric vehicles (EVs). In this scenario, the use of energy storage systems (ESSs) is becoming technologically attractive but problems of economic and ecological sustainability are still evident. For these reasons, II-Life battery modules are a possible solution for supporting power systems: they are a promising prospect for the modernization process. We propose a method to size an ESS of exhausted plug-in EV battery packs for grid support applications. The method estimates the residual value of cycles for II-Life battery modules, the decrease in the supplied power due to the battery ageing and the number of EV battery packs to meet service requirements. Then, an economic assessment is presented to compare them with an equivalent I-Life storage system.

1 INTRODUCTION

Energy storage systems (ESSs) for power system application is attracting significant interest and attention as an enabling solution for integrating the growing penetration of renewable energy resources and electric vehicles (EVs) into electrical grids, (Calderaro, 2014 – Tejada-Arango, 2018). Likely, ESSs are becoming an essential contributor to modernization investments of power systems at each voltage level. In fact, the ESSs can provide a technical solution to face current industry challenges such as power quality, network security, congestion management, generator's low utilization factor, and fuel price volatility. Consequently, the storage devices can propose ancillary services bringing benefits to customers and energy operators, (Grabert, 2017 – Ju, 2018).

However, two main challenges must be faced to support the integration of ESSs into the networks: the economic and ecological sustainability. Promising prospects are coming from the use of II-Life battery modules, reusing EV battery packs for alternative uses. In particular, they still have significant

remaining capacity for grid support applications, although this is not sufficient to provide an electric driving range. The main advantages of these battery modules are the supposed lower cost compared with new battery modules and the possibility to delay the development of the EV battery packs recycling chain (Viswanathan, 2011).

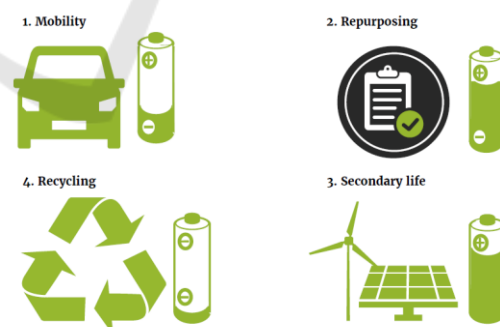


Figure 1: II-Life battery process, (Reid, 2016).

In the literature, the relationship between II-Life batteries and network electrical systems has been the subject of several recent investigations. The use of

^a <https://orcid.org/0000-0002-3474-2470>

^b <https://orcid.org/0000-0003-0868-6601>

^c <https://orcid.org/0000-0002-7768-7125>

^d <https://orcid.org/0000-0001-6405-7020>

II-Life battery-based ESSs for network support is recently analysed in several papers. In particular, in (Viswanathan, 2011) the authors propose a method for determining the optimal rating of the modules and the state of charge (SoC) profile during the operation. In (Saez-de-Ibarra, 2016), an optimization study is presented in order to maximize the value of an electric vehicle battery to be used as a transportation battery (in its first life) and, then, as a resource for providing grid services (in its second life). Also in (Lacey, 2013) II-Life batteries are used for provision of services with particular emphasis on peak shaving and upgrade deferral of low voltage (LV) distribution systems, while in (Gladwin, 2013) and (Koch-Ciobotaru, 2015) a general estimation of the use of batteries for electrical systems and a feasibility analysis are investigated, respectively. The integration of photovoltaic (PV) energy sources is proposed in (Mukherjee, 2015), where studies on the modular boost-multilevel buck converter to control the storage systems are proposed, and in (Gohla-Neudecker, 2015), where it is deduced an effective control strategy for attaining maximum system performance with minimum battery cell aging. Ref. (Strickland, 2014) and (Tong, 2015 – Hamidi, 2013) suggest a more general approach for supporting the integration of renewable energy resources. In (Saez-de-Ibarra, 2016) the important task of II-Life batteries sizing, is faced. It is a complex procedure due to many uncertainty factors such as degradation factors, calendar life, and applications.

With this in mind, here, we extend (Calderaro, 2017) by proposing a method to size the II-Life battery-based ESSs and assess the economic outcomes. The method is based on two main steps: the first one allows identifying an approximate value of the residual number of cycles and the maximum power that battery modules of II-Life ESS can deliver, whereas in the second one, we calculate the annual cost of energy to compare it with an equivalent I-Life storage system.

2 SIZING METHOD FOR II-LIFE BATTERIES

We propose a method for sizing an ESS consisting of II-Life lithium batteries. The method takes into account the real calendar life of the battery modules and the uncertainty related to the residual capacity measurements. The sizing methodology is composed of four steps:

- modelling of the II-Life battery model consisting of the series of a resistance and an ideal voltage source and their relationship with SoC and charging/discharging cycles (CDC);
- calculation of the residual cycles of the II-Life lithium batteries by linearizing the relationship between the batteries residual capacity and CDC;
- estimation of the II-Life battery aging in terms of supplied power by linearizing the relationship between the batteries internal resistance and CDC;
- Monte Carlo (MC) analysis to compute the number of II-Life battery modules according to the capacity and capability requirements.

2.1 II Life Battery Model

The II-Life battery is modelled as an ideal voltage source in series with a resistor. In particular, the ideal voltage source represents the open circuit voltage (OCV) depending on SoC of the battery module, while the series resistor R_{int} represents its overall internal resistance.

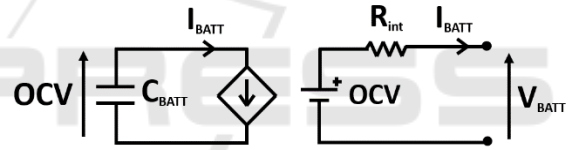


Figure 2: Proposed II-Life battery model.

The equations (1) describes the electric model of II-Life battery modules. Specifically, the first equation represents the Kirchoff's voltage law, while the second one is the n -polynomial relation between OCV and SoC. The third equation models the SoC update law, according to the required current from the battery modules.

$$\begin{cases} V_{BATT}(t) = OCV(t) - R_{int} I_{BATT}(t) \\ OCV(SoC) = \beta_n \cdot SoC^n + \beta_{n-1} \cdot SoC^{n-1} + \dots + \beta_0 \\ SoC(t) = SoC(t=0) + \frac{1}{3600 \cdot C_{BATT}} \int_0^t V_{BATT}(\tau) \cdot I_{BATT}(\tau) d\tau \end{cases} \quad (1)$$

In (1), $\beta_0 \dots \beta_n$ are the interpolation coefficients, I_{BATT} , V_{BATT} and C_{BATT} are the battery modules current, voltage, and capacity, respectively.

Moreover, battery-aging leads to a decrease in battery capacity as CDC increases described by the function f as follows:

$$C_{BATT} = f(CDC) \tag{2}$$

In Section 2.2, we present a method to estimate the function f starting from EV battery datasheet. In a similar way, the g function describes the increase of R_{int} by increasing CDC as follows:

$$R_{int} = g(CDC) \tag{3}$$

The method to estimate the function g is presented in Section 2.3.

2.2 Residual Capacity vs. CDC Approximation

Often, manufacturers do not provide any information about relationships between the battery residual capacity C_{BATT} and its maximum number of CDC performed at different depth of discharge (DoD) or they give only some curves at certain DoD. In the following, we describe a methodology to approximate this relationship at different DoD.

Figure 3 shows the typical trend (in logarithmic scale) between the calendar life in terms of maximum number of CDC and the DoD of a battery module (Julien, 2016). Generally, the functional dependency between CDC and DoD can be formalized by a test curve, a table, or a mathematical relationship based on measured data, which allows us to estimate the number of CDC before the battery module reaches its end of life (EoL). The EoL identifies the maximum acceptable reduction of the battery rated capacity and it is strongly dependent on the battery application (traction, energy, etc.).

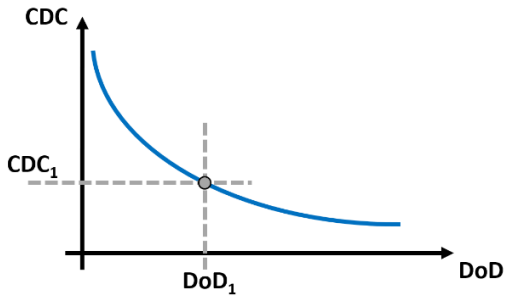


Figure 3: Lithium batteries typical trend - maximum number of CDC vs. DoD.

In Figure 4, we show the general trend of the relationship between the residual capacity C_{BATT} and the maximum number of CDC for a fixed value of DoD, which is given by the manufacturer (Julien, 2016). Typically, a nonlinear function describes this relationship for lithium batteries. We observe a rapid

decrease of the battery residual capacity in the first part of the characteristic, then, in the middle one, the trend is almost linear and it decreases very quickly at the end of the curve. The knee of the curve on the right of Figure 4 identifies the battery EoL for energy applications EoL_{en} (typical value 60 - 70% of C_{BATT} rated value) whereas the EoL for traction purposes is defined when the residual capacity is in the range of 80 - 85% of C_{BATT} rated value. For our purpose, it is not relevant to identify battery discharge profiles (such as DoD, CDC, etc.) before the point $EoL_{trac} - CDC_{trac}$ (i.e. the number of CDC at the EoL_{trac}).

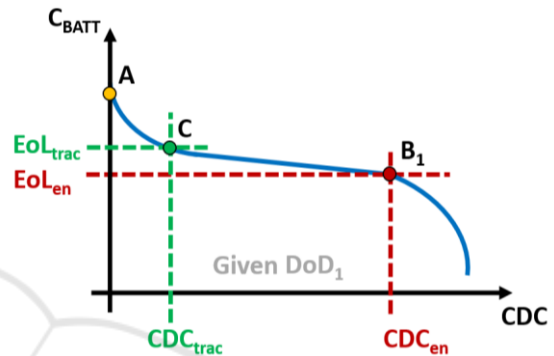


Figure 4: Lithium batteries typical trend - residual capacity vs. CDC.

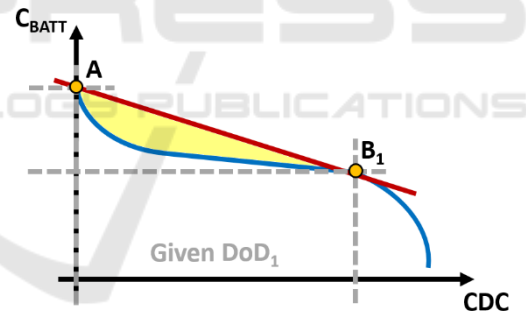


Figure 5: Linear approximation: residual capacity vs. CDC.

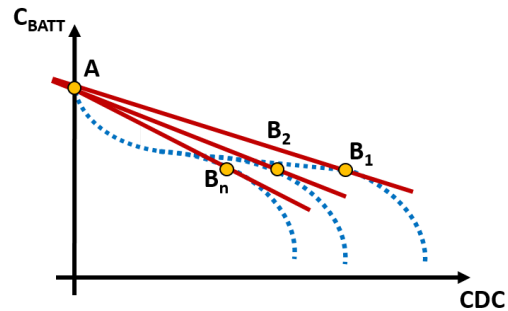


Figure 6: Linear approximation - residual capacity vs. CDC for different DOD values.

If the battery manufacturer does not give this curve, it is possible to take some assumptions to estimate the parameters of interest for our study. We use the following procedure to approximate the curve in Figure 4 by a line for different DoD values, as shown in Figure 5:

- select a DoD value from Figure 3 (DoD_1) to obtain a maximum number of CDC (CDC_1) that represents the number of cycles when the battery module reaches its energy EoL_{en} ;
- draw the point B_1 in the plane C_{BATT}/CDC (Figure 5);
- repeat the same procedure for each value of DoD in Figure 3 in order to obtain a set of $n-1$ maximum values ($CDC_2, CDC_3, \dots, CDC_n$) and for each maximum value of CDC, in the plane C_{BATT}/CDC draw the points (B_2, B_3, \dots, B_n) as show in Figure 6;
- in the plane C_{BATT}/CDC , identify the point A in correspondence of 0 cycles and C_{BATT} rated capacity;
- draw a line from the point A to each point $B_i, i=(1, 2, \dots, n)$; each line represents a specific DoD value (Figure 6);
- calculate the coefficients of the straight lines.

It is worth noting that the constellation of points ($B_1, B_2 \dots B_n$) defines different number of cycles at the energy EoL of the battery.

In particular, the yellow area in Figure 5 shows the error obtained by using the proposed linear approximation. It is greater in the I-Life of the battery, but it is not important for our methodology.

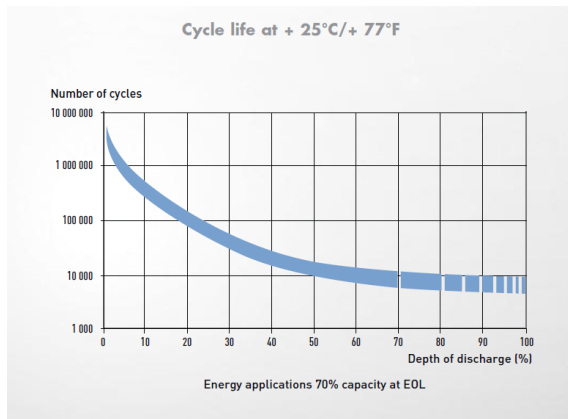


Figure 7: Maximum number of CDC vs. DoD trend for SAFT lithium-ion batteries.

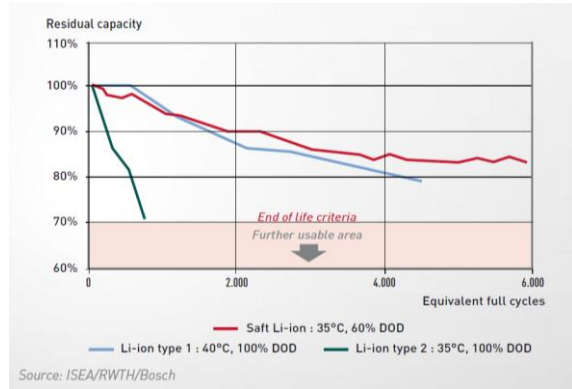


Figure 8: Residual capacity vs. CDC trend for SAFT lithium-ion batteries.

According to real data provided by batteries manufacturers (SAFT, 2014), and showed in Figure 7-8, the proposed linear approximation reasonably describes the relationship between residual capacity and the maximum number of CDC.

2.3 Aging of Internal Resistance Approximation

The internal resistance of Li-ion batteries also increases with use and aging. The increase in R_{int} leads to a reduction of the maximum power that the battery can deliver and therefore it is necessary to estimate this increase so that the ESS is able to supply the required power for a given grid service until its EoL. Unfortunately, manufacturers of EV batteries very often do not provide such information in datasheets.

In our analysis, we assume that the increase of the internal resistance during the battery life is a synchronous process with the reduction of its residual capacity.

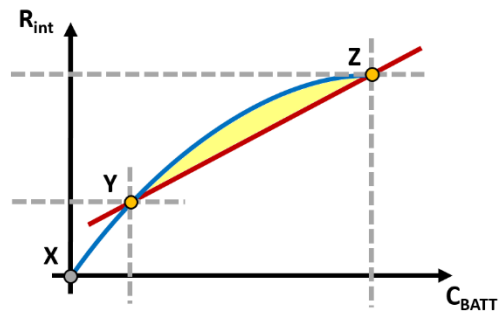


Figure 9: Internal resistance vs. Residual capacity: typical trend and linear approximation.

Figure 9 shows the typical trend of the internal resistance reducing the battery residual capacity (i.e. increasing the aging). In particular, the X, Y and Z points are defined by the pair of values R_{int} , C_{BATT} at the beginning of life (these values are provided by battery manufacturer), at the EoL for traction, and at the EoL for energy applications, respectively. The Y and Z points are very difficult to estimate because we usually do not have any data from the battery manufacturers.

We assume that the increase in the R_{int} is given by the ratio between the nominal capacity and the residual capacity of the battery. Therefore, to estimate the point Y (or Z) it is necessary to multiply the R_{int} nominal value (X point) for the ratio between battery nominal and residual capacity. Finally, established the Y and Z points, we can linearly estimate the trend of R_{int} with the aging. The yellow area in Figure 8 shows the error obtained by using the proposed linear approximation.

2.4 Equivalent Sizing of II-Life ESS

In order to size the II-life ESS (i.e. define the number of II-Life battery modules), we have to identify the service that the ESS must perform. Let us assume that this application has a fixed DoD (e.g. DoD_1).

The proposed procedure is based on a preliminary sizing obtained by using a conventional methodology computing the number of I-Life battery modules M , fixed the application (i.e. the necessary power and energy for the service, the DoD value and thus the maximum number of CDC). M is equal to the maximum value between the ratio of the energy requirement and the energy of one I-Life battery module, and the ratio of the power requirement and the power of one I-Life battery module. In order to consider the II-Life of the modules, we assume, for each one of them, a reduced capacity (battery capacity equal to the EoL_{trac} value multiplied C_{BATT}) and an increased R_{int} value: in this way, the number of II-Life modules is greater than the one obtained by using I-Life battery modules.

Afterwards, we bring into the problem the uncertainties due to an incorrect estimation of the residual capacity and maximum power. We assume M as the number of II-Life battery modules needed for the application in case of uncertainty is not considered. According to the available data, it is possible to consider the points B_1 , C and Z as random variables with a given probability distribution (e.g., uniform, Gaussian, etc.) to in order to bring into account their uncertainties. We use a MC approach to calculate: i) a distribution of residual cycles of II-Life

battery for the application; ii) a distribution of battery maximum power at the EoL for the application.

We assume for our studies two Gaussian distributions ($\mu_1=CDC_{trac}$, $\sigma_1=1$, $\mu_2=CDC_{en}$ and $\sigma_2=1$), to tackle the uncertainty due to a wrong estimation of points B_1 and C . In a similar way, a Gaussian distribution ($\mu_Z=1.66*R_{int}$, $\sigma_Z=1$) is assumed at the point Z .

For these reasons, we consider m II-Life battery modules in addition to M , able to guarantee a number of CDC equal to $CDC^* \geq CDC_{trac} - CDC_{en}$, and maximum battery power at EoL_{en}, $P_{BATT} \geq P^*$. In such a way, the remaining life of the II-Life ESS and its maximum power at the EoL_{en} can be designed. In particular, we introduce m_1 and m_2 that represent the additional capacity necessary to the II-Life ESS for satisfying the required CDC and the additional power necessary for satisfying the maximum required power, respectively. We calculate the parameter m_1 and m_2 by implementing an iterative procedure based on a MC approach. Our procedure starts with $m_1=m_2=0$ and ends when it finds the smaller value of m_1 that ensures

$$\Pr(CDC \text{ of } M \text{ modules} \geq CDC^* \mid M+m_1 \text{ modules}) > \alpha_{90\%} \quad (4)$$

and the smaller value of m_2 that ensures

$$\Pr(P_{BATT} \text{ of } M \text{ modules} \geq P^* \mid M+m_2 \text{ modules}) > \alpha_{90\%} \quad (5)$$

where $\alpha_{90\%}$ is the percentile of the resulting distribution.

The number m of battery modules satisfying the CDC^* and the P^* requirements is the maximum value between m_1 and m_2 . Then, we are able to define the final number of II-Life battery modules ($M+m_i$ with $i=1$ or 2 depending on the m_i maximum value) necessary to achieve an equivalent I-Life ESS and to perform an economic assessment.

3 ECONOMIC METRIC

We use the net present value (NPV) as economic metric to examine costs and revenues while accounting for the time value of money (Masters, 2013). If the NPV of a system is positive, then the investment should be profitable. A negative NPV indicates that the returns are worth less than the cash outflows and the investment does not show a financial benefit, although unquantified benefits may be present. Annual cost of energy (ACOE) in [\$/year] represents the present value of total cost C_{tot} multiplying by the capital recovery factor CRF . The CRF converts a present value into a stream of equal

annual payments over a specified lifetime N [year], at a specified interest rate r . It is defined as follows:

$$CRF = \frac{r(1+r)^N}{(1+r)^N - 1} \quad (6)$$

and the C_{tot} is given by:

$$C_{tot} = (C_I + C_{M\&O} + C_{REP}) \quad (7)$$

where C_I is the storage capital cost, $C_{M\&O}$ is the net present value of the total operations and maintenance costs and C_{REP} is the present value of the replacement costs.

The capital cost C_I is the one-time investment, which brings the ESS into an operable status. It contains two subsystems: the first one is the power sub-system whereas the second one is the energy storage sub-system. The cost of the two sub-systems should be added together to get the overall capital cost. C_I can be formulated as

$$C_I = C_P P_R + C_E E_R + C_{FC} \quad (8)$$

where P_R [kW] and E_R [kWh] are the ESS rated power and capability; C_P [\$/kW] and C_E [\$/kWh] are the specific costs mainly related to the electronic interface to the network and to the size of the ESS, respectively. C_{FC} [\$] is the fixed cost (building cost, landing cost, construction cost, etc.).

There are at least four elements in the $C_{M\&O}$ cost: 1) labour associated with plant operation, 2) plant maintenance, 3) equipment wear leading to its loss-of-life, and 4) disposal and decommissioning cost. The $C_{M\&O}$ cost is defined as follows:

$$C_{M\&O} = \sum_{n=1}^N \frac{C_n}{(1+r)^n} \quad (9)$$

where C_n [\$] is the annual operation cost on n years and it is defined as a function of two main parts: a fixed one related to the ESS rated power, and a variable part depending on its annual discharged energy E_{year} [kWh].

$$C_n = C_f P_R + C_v E_{year} + C_r \quad (10)$$

$$C_r = \frac{E_{year}}{\eta_{CH}} C_{CH}$$

The annual operation cost is split in variable cost (C_v) and charging cost (C_r): where η_{CH} is the battery charging efficiency and C_{CH} [\$/kWh] is the electricity cost coefficient for charging the ESS.

Battery modules have to be replaced one or more times during the project lifetime. The NPV of replacement cost is:

$$C_{REP} = C_{RP} [(1+r)^{-L} + (1+r)^{-2L} + \dots] \quad (11)$$

where C_{RP} [\$] is the future value of replacement cost and L is the replacement period that can be estimated by using the battery modules datasheet such as (Julien, 2016).

4 SIMULATION FRAMEWORK

We apply the introduced methodology for the sizing of II-Life ESSs to a real distribution system. We consider the implementation of a peak shaving service for the microgrid that supplies the Campus of the University of Salerno (UniSA).

4.1 Case Study

The UniSA microgrid is a 12 bus 20 kV distribution system with two feeders configured in closed loop (Figure 10). Connected to the grid, there are several distributed generators (DG). Two combined heat and power (CHP) units, with a rated power of 580 kW each one at bus 11, and eight PV power plants for a total PV rated power of 1076 kW installed on the roof of the campus buildings (bus 2, 3, 4, 5, 6, 8, 9 and 12). CHP units produce both electricity used to supply the loads and thermal energy used to heat water of the campus sport facilities.

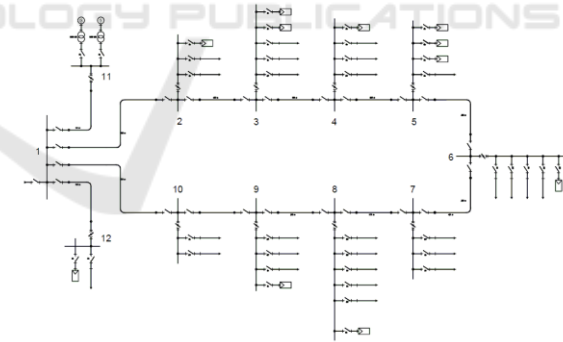


Figure 10: Power grid of the UniSa Campus.

In Figure 11, we show the typical daily profiles of the net active power drawn from the main external PCC by the UniSA network (bus 1). Blue and green lines depict the active power absorption with and without internal PVs and CHPs, respectively. Finally, yellow and pink lines show the average (calculated every 15 minutes) active power generated by the PV and CHP units.

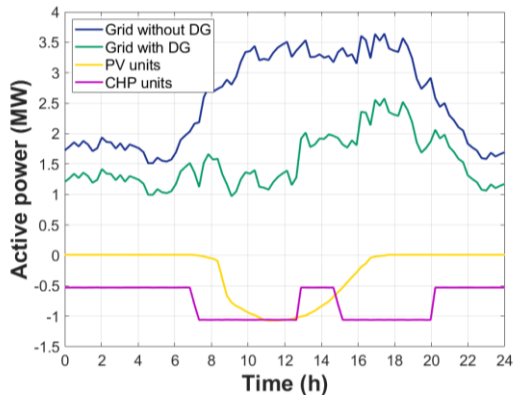


Figure 11: Active power drawn from the UniSA microgrid.

Furthermore, the study in (Graber, 2017), based on the CO.S.MO. (*Cooperative Systems for Sustainable Mobility and Energy Efficiency*) European research project, allows us to consider the additional demand due to the connection of EVs to charging stations (CSs) into the Campus.

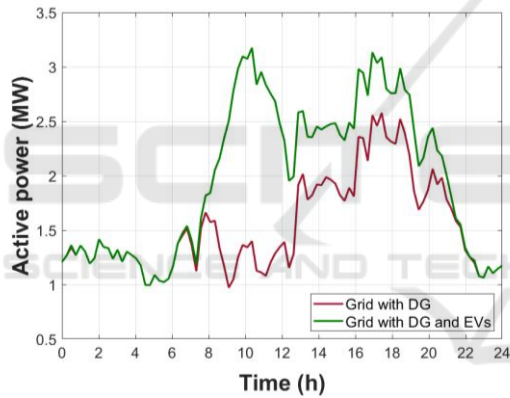


Figure 12: Active power drawn from the UniSA microgrid by adding the EVs charging load.

The study assumes that the users behaviour and their mobility needs highlighted by the COSMO data analysis, do not change moving from ICE-based (internal combustion engine) vehicles to battery EVs. Moreover, different types of CSs (AC level 2, CHAdeMO, SAE Combo, Tesla Supercharger, etc.), each of them characterized by different values of charging power, are considered in the analysis. EV charging demand profile is depicted in Figure 12.

4.2 Economic Assessment

We consider one II-Life battery ESS supporting CSs in the UniSA parking area and implementing a peak shaving based control. More in detail, during the day, the ESS acts when the power demand of the UniSA

Campus is greater than a given threshold working in load following mode. At night, the ESS charge itself in constant charging power mode.

In our analysis, we consider two different size of the ESS according to the imposed maximum power drawn from the main external grid, P_{max}^G . More in detail, by imposing $P_{max}^G=3.00$ MW we need an ESS of 0.55 MW, 1.6 MWh (ESS₁), while by imposing $P_{max}^G=2.75$ MW we need an ESS of 0.80 MW, 2.0 MWh (ESS₂), (Graber, 2017).

Figure 13 shows the flattening effect of the II-Life battery ESSs on the UniSA power demand when the electric load is greater than P_{max}^G . The results for the $P_{max}^G=3.00$ MW and $P_{max}^G=2.75$ MW case studies are presented. In particular, the ESS reduces the peak load acting in load following mode from 9:00 a.m. to 12:00 p.m. and from 16:00 p.m. to 19:00 p.m., while the ESS charges itself from the external grid in constant power mode, from 21:00 p.m. to 7:00 a.m.

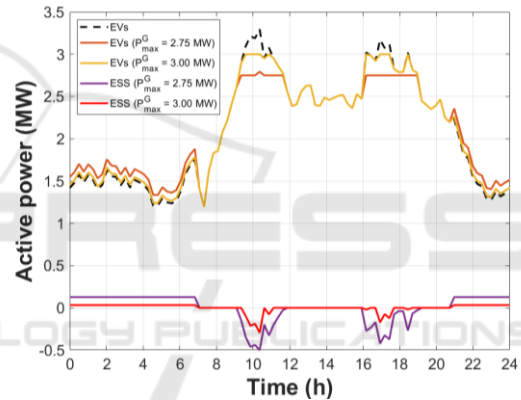


Figure 13: Daily trends of active power drawn by UniSA Campus from the external grid with EVs charging load and second life ESS.

Table 1: Parameter for the Economic Assessment.

| Parameter | Value | Unit |
|------------------------|--------|--------|
| N | 20 | Years |
| r | 4 | % |
| C_P | 125 | \$/kW |
| C_E | 470 | \$/kWh |
| C_f | 9.2 | \$/kW |
| C_v | 0.0011 | \$/kWh |
| $E_{year\ for\ ESS_1}$ | 440 | MWh |
| $E_{year\ for\ ESS_2}$ | 550 | MWh |
| C_{CH} | 0.114 | \$/kWh |

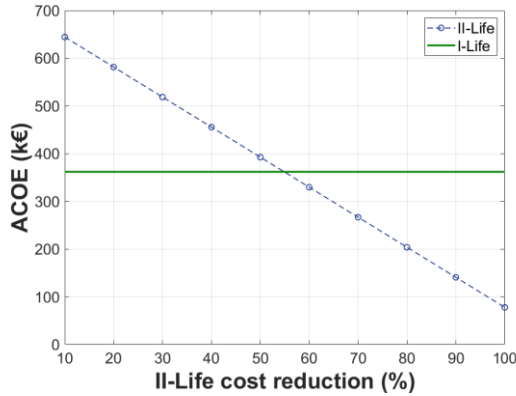


Figure 14: Comparison of ACOE for I-Life and II-Life battery ESS.

We calculate the ACOE for I-Life and II-Life battery solutions based on the parameters in Table 1. We, also, assume that C_{FC} is zero and the C_{REP} is equal to 80% of C_l .

In Figure 14, we compare the ACOE of the I-Life ESS and that of the II-Life ESS, assuming the $P_{max}^G=3.00$ MW case study. The aim is to give a competitive price to the II-Life ESS compared to the I-Life solution. In our case study, the sensitivity analysis has pointed out that the price of II-Life battery modules should be reduced at least of 55% compared to the I-Life battery modules, in order to obtain an ACOE value for the II-Life ESS comparable to that of the I-Life ESS. It is worth to note that 100% cost reduction of II-Life battery modules leads to an ACOE of the II-Life ESS not equal to zero due to O&M costs.

Table 2: II-Life ESS Sizing by using Different Battery Packs (0.55 MW, 1.6 MWh).

| Model | Module energy | Module power | M | m_1 | m_2 |
|----------------------|---------------|--------------|-----|-------|-------|
| <i>Nissan leaf</i> | 24 kWh | 90 kW | 67 | 15 | 3 |
| <i>Tesla Model S</i> | 75 kWh | 285 kW | 22 | 5 | 1 |
| <i>BMW i3</i> | 33 kWh | 125 kW | 49 | 11 | 2 |
| <i>Renault Zoe</i> | 22 kWh | 65 kW | 73 | 16 | 4 |
| <i>Citröen CO</i> | 14 kWh | 49 kW | 114 | 25 | 6 |

Table 3: II-Life ESS Sizing by using Different Battery Packs (0.8 MW, 2.0 MWh).

| Model | Module energy | Module power | M | m_1 | m_2 |
|----------------------|---------------|--------------|-----|-------|-------|
| <i>Nissan leaf</i> | 24 kWh | 90 kW | 84 | 19 | 4 |
| <i>Tesla Model S</i> | 75 kWh | 285 kW | 27 | 6 | 2 |
| <i>BMW i3</i> | 33 kWh | 125 kW | 61 | 14 | 3 |
| <i>Renault Zoe</i> | 22 kWh | 65 kW | 91 | 20 | 5 |
| <i>Citröen CO</i> | 14 kWh | 49 kW | 143 | 32 | 8 |

In Table 2, we show the number of I-Life battery modules (M) and II-Life battery modules (M plus the maximum value between m_1 and m_2) needed to satisfy the load following application ($P_{max}^G=3.00$ MW case study) and whose economic evaluation is shown in Figure 13. The number M , m_1 , and m_2 are calculated by using different EV battery packs of the best-selling EV models for tackling the uncertainty due to residual capacity estimation and increase of the internal resistance. A similar analysis is carried out for the $P_{max}^G=2.75$ MW case study and it is proposed in Table 3. It is worth to note that the additional II-Life battery modules needed to satisfy the power requirement of the peak shaving service is always less binding than that concerning the maximum number of CDC requirement.

5 CONCLUSIONS

We present a sizing method for the economic assessment of II-Life ESSs in providing energy services. A linear approximation is assumed to deal with the degradation and aging of lithium-ion batteries. We propose a methodology to calculate the number of battery modules able to guarantee the power service requirements at the EoL for energy applications and to tackle the uncertainty due to the estimation of the residual capacity in II-Life batteries.

We calculate the ACOE of two different II-Life battery solutions able to provide a peak shaving service on the UniSa Campus MV network by reducing the imposed maximum power drawn from the main external grid. We compare them with the I-Life ESS in order to identify a competitive price of II-Life battery modules.

ACKNOWLEDGEMENTS

The authors gratefully thank UE and all technological partners who have contributed to the success of the CO.S.MO. research project.

REFERENCES

- Tejada-Arango, D. A., Domeshek, M., Wogrin, S., Centeno, E., 2018. Enhanced Representative Days and System States Modeling for Energy Storage Investment Analysis. In *IEEE Transactions on Power Systems*, vol. 33, pp. 6534-6544.
- Ju, C., Wang, P., Goel, L., Xu, Y., 2018. A Two-Layer Energy Management System for Microgrids with

- Hybrid Energy Storage Considering Degradation Costs. In *IEEE Transactions on Smart Grid*, vol. 9, pp. 6047-6057.
- Calderaro, V., Galdi, V., Graber, G., Graditi, G., Lamberti, F., 2014. Impact assessment of energy storage and electric vehicles on smart grids. In *Proc. Electric Power Quality and Supply Reliability Conf.*, pp 15-18.
- Graber, G., Lamberti, F., Calderaro, V., Galdi, V., Piccolo, A., 2017. Stochastic characterization of V2G parking areas for the provision of ancillary services. In *Proc. Innovative Smart Grid Technologies Conf. Europe*, pp.1-6.
- Viswanathan, V. V., Kintner-Meyer, M., 2011. Second Use of Transportation Batteries: Maximizing the Value of Batteries for Transportation and Grid Services. In *IEEE Trans. Vehicular Technology*, vol. 60, pp. 2963-2970.
- Saez-de-Ibarra, A., Martinez-Laserna, E., Stroe, D., Swierczynski, M., Rodriguez, P., 2016. Sizing Study of Second Life Li-ion Batteries for Enhancing Renewable Energy Grid Integration. In *IEEE Trans. on Industry Applications*, vol. 52, pp. 4999-5008.
- Lacey, G., Putrus, G., Salim, A., 2013. The use of second life electric vehicle batteries for grid support. In *Proc. IEEE EUROCON Conf.*, pp. 1255-1261.
- Gladwin, D. T., Gould, C. R., Stone, D. A., Foster, M. P., 2013. Viability of "second-life" use of electric and hybrid electric vehicle battery packs. In *Proc. IECON Industrial Electronics Society Conf.*, pp. 1922-1927.
- Koch-Ciobotaru, C., Saez-de-Ibarra, A., Martinez-Laserna, E., Stroe, D. I., Swierczynski M., Rodriguez, P., 2015. Second life battery energy storage system for enhancing renewable energy grid integration. In *Proc. Energy Conversion Congress and Exposition Conf.*, pp. 78-84.
- Mukherjee N., Strickland, D., 2015. Control of Second-Life Hybrid Battery Energy Storage System Based on Modular Boost-Multilevel Buck Converter. In *IEEE Trans. on Industrial Electronics*, vol. 62, pp. 1034-1046.
- Gohla-Neudecker, B., Bowler M., Mohr, S., 2015. Battery 2nd life: Leveraging the sustainability potential of EVs and renewable energy grid integration. In *Proc. Clean Electrical Power Conf.*, pp. 311-318.
- Strickland, D., Chittock, L., Stone D. A., Foster, M. P., Price, B., 2014. Estimation of Transportation Battery Second Life for Use in Electricity Grid Systems. In *IEEE Trans. on Sustainable Energy*, vol. 5, pp. 795-803.
- Tong, S., Fung T., Park, J. W., 2015. Reusing electric vehicle battery for demand side management integrating dynamic pricing. In *Proc. IEEE Smart Grid Communications Conf.*, pp. 325-330.
- Hamidi, A., Weber L., Nasiri, A., 2013. EV charging station integrating renewable energy and second-life battery. In *Proc. Renewable Energy Research and Applications Conf.* pp. 1217-1221.
- Julien, C., Mauger, A., Vijn, A., Zaghbi, K., 2016. Lithium Batteries - Science and Technology. Springer, 1st edition.
- SAFT, May 2014. Lithium-ion battery life. Document N°21893-2-0514 [Online]. Available: http://www.saftbatteries.com/force_download/li_ion_battery_life_TechnicalSheet_en_0514_Protected.pdf&prev=search
- Masters, G., 2013. Renewable and Efficient Electric Power Systems. Wiley, 2nd edition.
- Calderaro, V., Galdi, V., Graber, G., Massa, G., Piccolo, A., 2014. Plug-in EV charging impact on grid based on vehicles usage data. In *Proc. International Electric Vehicle Conf.*, pp. 1-7.
- Calderaro, V., Galdi, V., Graber, G., Lamberti, F., Piccolo, A., 2017. A sizing method for economic assessment of II-life batteries for power system applications. In *Proc. Power & Energy Society General Meeting*, pp.1-5.
- Graber, G., V., Galdi, Calderaro, V., Mancarella, P., 2017. A stochastic approach to size EV charging stations with support of second life battery storage systems. In *Proc. IEEE Manchester PowerTech*, pp.1-6.
- Reid, G., Julve, J., 2016. Second Life-Batteries as Flexible Storage for Renewables Energies. Report. [Online]. Available: https://www.bee-ev.de/fileadmin/Publikationen/Studien/201604_Second_Life-Batterien_als_flexible_Speicher.pdf
- Thirugnanam K., Kerk S. K., Yuen C., Liu N., Zhang M., 2018. Energy Management for Renewable Micro-Grid in Reducing Diesel Generators Usage with Multiple Types of Battery. In *IEEE Transactions on Industrial Electronics*, vol. 65, pp. 6772-6786.